D.C. Nascimento and J.C. da S. Lacava

Design of Arrays of Linearly Polarized Patch Antennas on an FR4 Substrate

Design of a probe-fed electrically equivalent microstrip radiator.

A new strategy for designing probe-fed electrically equivalent microstrip radiators based on their electrical dimensions is discussed in this article. Radiators on a Flame Retardant 4 (FR4) substrate are synthesized for equivalent performance, aiming at lower H-plane cross polarization over the bandwidth and resistive input impedance at the operating frequency. The effect of mutual coupling is analyzed for two classical arrangements: side-by-side and collinear configurations. With the proposed strategy, a broadside collinear array of linearly polarized rectangular patches is designed to operate at the center frequency of the industrial, scientific, and

Digital Object Identifier 10.1109/MAP.2015.2453916
Date of publication: 24 August 2015

BACKGROUND IMAGE © ISTOCKPHOTO.COM/ FTOTTI1984

medical (ISM) band (2.45 GHz) on a moderately thick FR4 substrate. The array is designed for low cross polarization in the H-plane and to comply with the specified directivity and side lobe level (SLL). Special attention to the beamforming circuit design leads to a radiation efficiency near 70%.

MICROSTRIP ANTENNAS

Microstrip antennas have become customary components in modern communications systems, including aerospace and biomedical applications [1], [2]. This wide diversity is mainly due to their peculiar characteristics, such as low weight, small volume, and compatibility with integrated circuits at microwave frequencies. Another important advantage is the ability to conform their low profile to curved surfaces, thus uniquely meeting mechanical and aerodynamical needs [3].

A conventional microstrip antenna comprises a conductive patch, which may assume different forms, printed on top of a thin grounded dielectric. From the various antenna-feeding techniques developed over the years [1], this article covers the typical coaxial probe feeding, such as the practical SubMiniature Version A (SMA) connector. However, this basic structure can only handle low power and operate over a narrow frequency range, the latter being regarded as its most severe constraint. A simple intuitive way to overcome these limitations would be the use of thick substrates, except that this leads to the excitation of surface waves, thus substantially decreasing the antenna radiation efficiency [1], [2]. A thick-substrate probe-fed antenna, either linearly or circularly polarized, designed according to the standard procedure [4], presents a highly inductive input impedance, so it is not properly matched to a 50-Ω SMA connector. Various techniques to compensate for the probe's inductive reactance have been proposed [5]–[13], but those solutions add greater complexity to the design and manufacture of the antenna. To overcome these limitations, two efficient design techniques for probe-fed, moderately thick microstrip antennas were recently proposed [14]–[17], permitting the accurate design of linearly and circularly polarized microstrip antennas based only on their intrinsic characteristics, without any external matching network.

Currently, to achieve higher levels of radiation efficiency (over 80%), antennas have to be designed on low-loss microwave laminates, with a loss tangent of about 0.002. Now that both the market and the technology are ready for mass production [18], cost-effective designs of microstrip antennas manufactured on a low-cost FR4 substrate were reported in [18]–[26]. Unfortunately, the FR4 substrate introduces additional complexity to the antenna design [18], [27]–[30], not only for the inaccuracy of its actual relative permittivity but also mainly to its considerable loss tangent (around 0.02). Variations in FR4 permittivity can shift the operating frequency, whereas the high loss tangent affects the antenna bandwidth and gain, resulting in poor radiation efficiency, as low as 30% (at 1.6 GHz, on a 1.5-mm thick substrate) [30]. To improve this relevant parameter, antennas have been manufactured on suspended FR4 substrates [18], [31]–[32] or on thicker single-layer FR4 substrates [30]. The side effect, however, is the degradation of their radiation performances. Usually, the cross-polarization level in the H-plane (CPLH-P) increases substantially, limiting the design of phased arrays [33]. To alleviate this unwanted effect, different techniques have been employed: typically, dual-probe feeding [34], a horizontal probe-fed half-wavelength strip combined with two vertical segments [33], and a defected ground structure [35]. However, these solutions (as well as the use of suspended substrates and techniques to compensate for the inductive reactance of the probe [5]–[13]) add, as mentioned previously, greater complexity to the antenna design and manufacture, hindering its industrial scale production where simple, cost-effective projects are preferred. Thus, rather than using the aforementioned strategies, this article covers the design and implementation of probe-fed single-layer antennas on moderately thick FR4 substrates. Using this method, antenna radiation efficiency near 70% (at 2 GHz) is achieved for a 6.0-mm-thick FR4 substrate [30].

A single radiating element cannot generally comply with the stringent requirements and protocols of modern communication systems [15]. Therefore, antenna arrays are used, provided that the appropriate choices of the radiating elements, their relative displacement, and the amplitude and phase of the excitation currents are made. The usual methodology for the analysis of antenna arrays made up of identical elements is the well-known pattern multiplication [36]. This methodology intrinsically assumes that the single-element radiation pattern is not modified by the mutual coupling between the array elements, in which case the radiators are classified as well-behaved [37]. Microstrip arrays on an infinite ground plane (as usually assumed in the preliminary design phase) can be fairly analyzed according to this methodology. However, from a practical point of view, the design of microstrip arrays is more complex since both the mutual coupling between the array elements and the finite dimensions of the grounded dielectric layer should be taken into account [38]. In addition, the design of linearly polarized arrays on the FR4 substrate must incorporate an efficient strategy to compensate for the high CPLPH-P, since good radiation efficiency requires a moderately thick substrate. Geometries with low mutual coupling are potential candidates for phased arrays [39].

Results for the mutual impedance between microstrip antennas can be found in many publications, specifically in those dedicated to array design [1], [38], [39]. However, these results do not permit a categorical comparison among their mutual coupling levels since the calculations do not use the same criterion. To overcome this limitation, a new design procedure is proposed for probe-fed linearly polarized (LP) electrically equivalent microstrip antennas printed on an FR4 substrate, resulting in lower levels of cross polarization in the antenna H-plane, all over the bandwidth. Therefore, the purpose of this article is to present a low-cost linear array composed of elements designed according to this new procedure. The first step is the determination of the patch geometry, considering the array has to comply with the following specifications over the ISM band (2.4–2.5 GHz): a 12-dB directivity in the broadside configuration, a −17-dB SLL, a −10-dB reflection coefficient magnitude, and the CPLH-P as low as −20 dB.

The experimental results for radiation patterns, CPLH-P, and reflection coefficient magnitude validate the proposed approach.

NEW DESIGN PROCEDURE

A simple and efficient strategy for designing electrically equivalent microstrip antennas based on their electrical dimensions was recently proposed in [40]. Following this strategy, radiators with rectangular (Figure 1), elliptical (Figure 2), and triangular (Figure 3) patches, printed on a square (100 mm × 100 mm) grounded FR4 substrate ($\varepsilon_r = 4.2$ and $\tan\delta = 0.02$) and fed by a 1.3-mm diameter coaxial probe, were designed [using the High Frequency Structure Simulator (HFSS) package [41]] at 2.45 GHz to comply with the ISM band (2.4–2.5 GHz). For a good radiation efficiency (over 75%), a 6.6-mm moderately thick substrate was used. The patch dimensions are shown in Figures 1–3.

According to this strategy, all three antennas exhibit the same 5.9% bandwidth (145 MHz at 10-dB return loss criterion) complying with the ISM band (100 MHz). Additional comparisons of the antennas are presented in Table 1. As seen, the radiation efficiency and directivity of the antennas are comparable. The directivity equivalence is explained by the similarity among the copolarized radiation patterns.

One notices, however, a large difference in the cross-polarized radiation [40]. To illustrate these effects, HFSS simulations are shown in Figures 4 and 5. H-plane normalized radiation patterns are shown in Figure 4, whereas the frequency behavior of the CPLH-P is presented in Figure 5. The CPLH-P changes substantially over the antenna bandwidth. The ΔCP parameter, which characterizes the

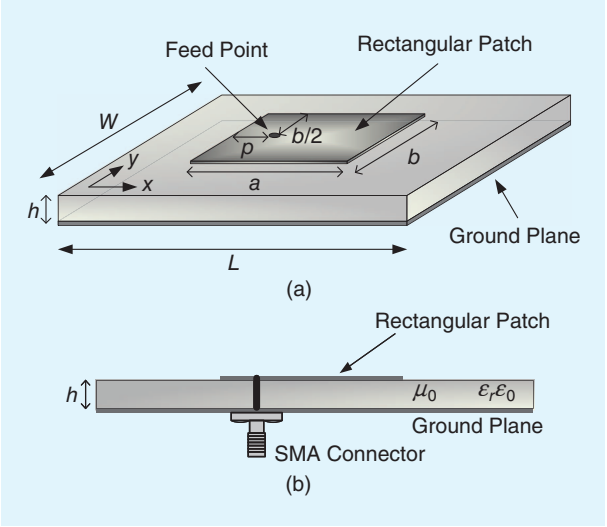

FIGURE 1. The probe-fed rectangular-patch LP antenna. $a = 26.75$ mm, $b = 21.45$ mm, and $p = 8.2$ mm. (a) Top view. (b) Side view.

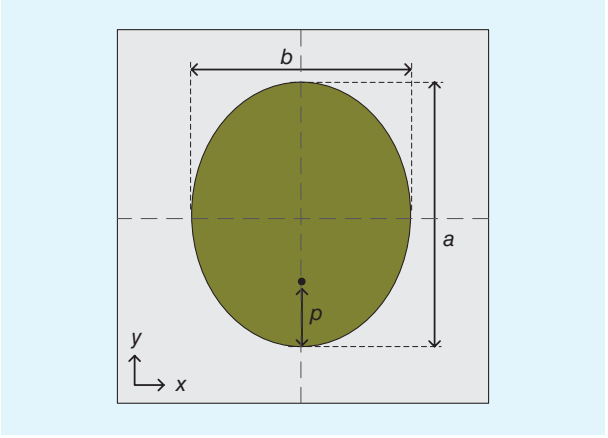

FIGURE 2. The probe-fed elliptical-patch LP antenna. $a = 32.55$ mm, $b = 18.9$ mm, and $p = 11.5$ mm.

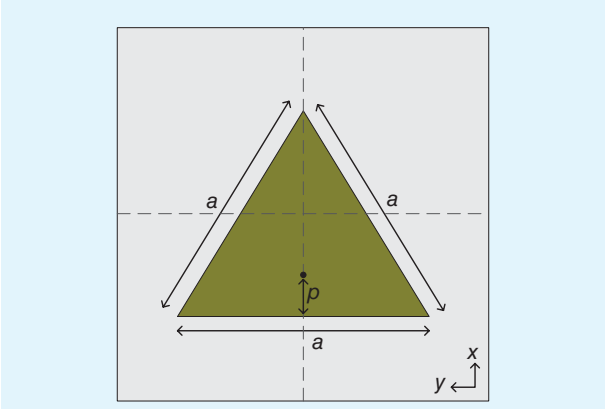

FIGURE 3. The probe-fed triangular-patch LP antenna. $a = 36.63$ mm and $p = 3.6$ mm.

TABLE 1. THE ELECTRICAL CHARACTERISTICS OF THE LP MICROSTRIP ANTENNAS.

	Rectangular	Elliptical	Triangular
Directivity (dB)	6.62	6.56	6.60
Radiation Efficiency (%)	78.4	77.2	76.7
Z_{in} (Ω)	50	50	50
CPLH-P (dB)	−18.6 ($\theta = 50°$)	−19.5 ($\theta = 50°$)	−12.6 ($\theta = 45°$)
ΔCP (dB)	−16.0– −20.7	−16.9– −21.7	−10.2– −15.2

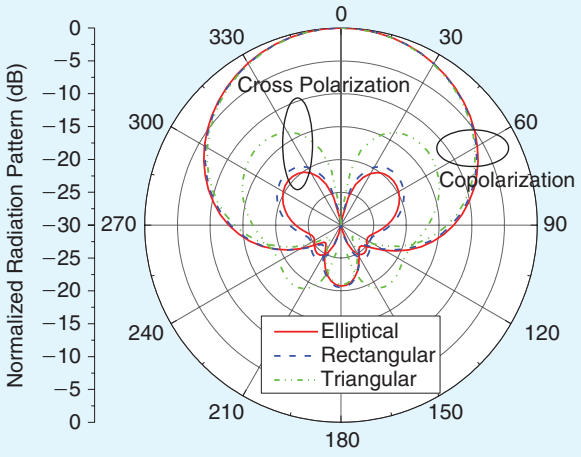

FIGURE 4. The H-plane normalized radiation pattern at 2.45 GHz.

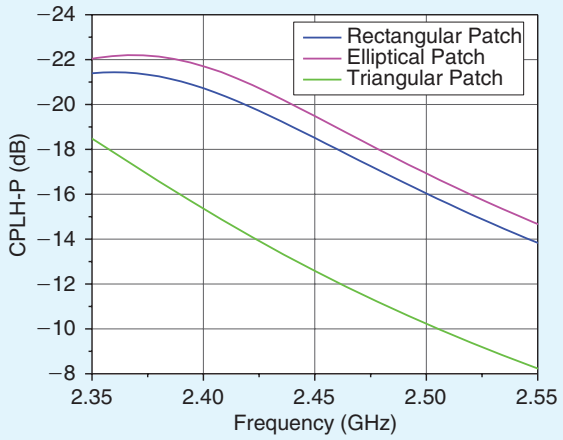

FIGURE 5. The H-plane cross-polarization level.

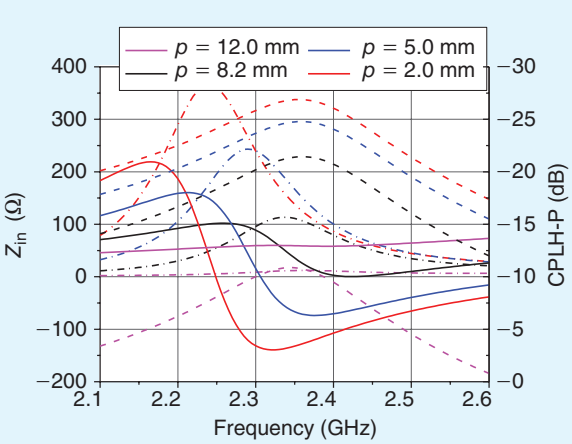

FIGURE 6. The rectangular patch. CPLH-P (--). Re [Z_{in}] (---). Im [Z_{in}] (—).

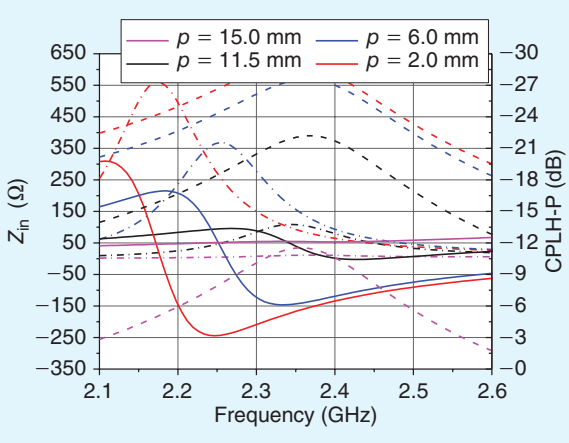

FIGURE 7. The elliptical patch. CPLH-P (--). Re [Z_{in}] (---). Im [Z_{in}] (—).

maximum-to-minimum variation of CPLH-P over the operating band, is also presented in Table 1.

Following the strategy proposed in [40], radiators can be designed for equivalent performance in terms of bandwidth and copolar radiation patterns but with no control of CPLH-P. To improve this strategy, the H-plane cross-polarization characteristics of the previous antennas were analyzed, aiming at lower CPLH-P over the antenna bandwidth and resistive input impedance at the operating frequency. The starting point was the well-known fact that the cross-polarization level of a rectangular patch is a function of the probe position [42]. To visualize this peculiar behavior, the probe position p was gradually reduced from the center to the edge of the patch. The graphics of input impedance and CPLH-P are shown in Figures 6–8.

Figures 6 and 7 show, for rectangular and elliptical patches, CPLH-P decreases with p and the shape of the cross-polarization curves is independent of frequency. Also, the lowest cross-polarization level does not occur at the operating frequency (2.45 GHz). Moreover, the reactance null shifts in frequency with the change of probe position p. On the other hand, large variations of CPLH-P for the triangular patch are shown in Figure 8. The analysis of these behaviors shows that it is possible to establish a particular condition for low CPLH-P all over the antenna bandwidth. For rectangular and elliptical patches, this condition results from a predesign focused on the

CPLH-P curves. This approach guarantees the best level of the CPLH-P curve at the desired frequency, regardless of the value of p. The design is completed by changing the position p for the zero reactance condition [30] at that frequency.

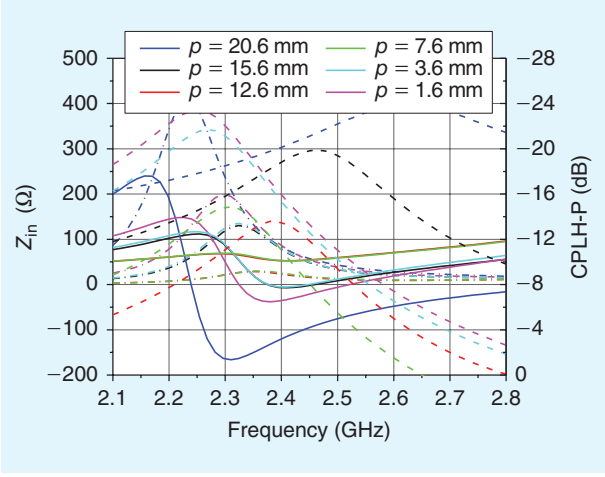

FIGURE 8. The triangular patch. CPLH-P (--). Re [Z_{in}] (---). Im [Z_{in}] (—).

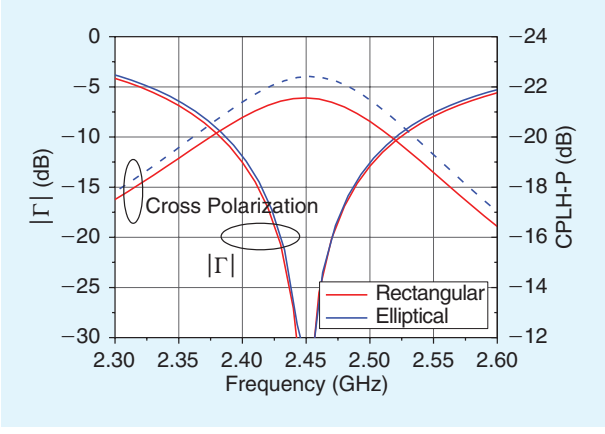

FIGURE 9. The reflection coefficient magnitude and CPLH-P of the rectangular and elliptical patches.

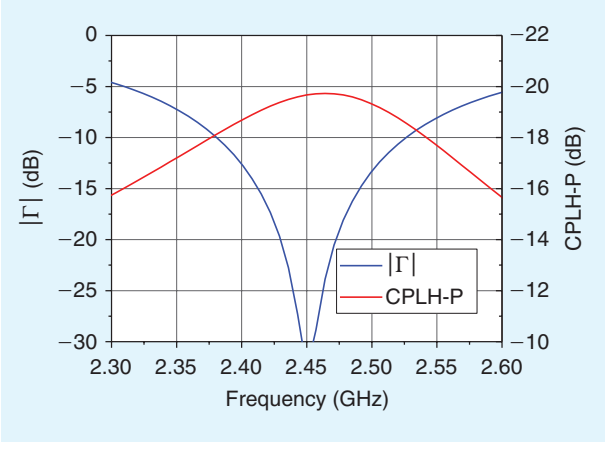

FIGURE 10. The reflection coefficient magnitude and CPLH-P of the triangular patches.

Applying this procedure to the previous radiators, the following new dimensions were obtained for the rectangular patch: $a = 25.6$ mm, $b = 20.5$ mm, and $p = 7$ mm. Note these new dimensions are close to those from the former strategy [40], $a = 26.75$ mm, $b = 21.45$ mm, and $p = 8.2$ mm, as shown in Figure 1. The same was found for the elliptical patch: $a = 31.2$ mm, $b = 18.25$ mm, and $p = 10.20$ mm, close to the previous dimensions, $a = 32.55$ mm, $b = 18.9$ mm, and $p = 11.5$ mm (Figure 2). In both cases, the input impedance at the operating frequency (2.45 GHz) is now real, approximately 130 Ω. This value was used to calculate the reflection coefficient magnitudes shown in Figure 9.

The triangular patch design is slightly more complex, since both the input reactance and cross-polarization curves shift in frequency as the probe position p changes. Using HFSS, such that the zero reactance condition occurs at the frequency where cross polarization is minimal, the following dimensions were obtained: $a = 35.7$ mm and $p = 15.6$ mm (versus $a = 36.63$ mm and $p = 3.6$ mm from the previous strategy; note that the value of p changed substantially to minimize the cross polarization). In this case, the antenna input impedance at the low-cross-polarization frequency is 50 Ω. This value was used to calculate the reflection coefficient magnitude shown in Figure 10.

As expected, using the new procedure, the CPLH-P parameter is quite stable over the operating band (Figures 9 and 10), unlike the parameter shown in Figure 5. The rectangular patch CPLH-P is –19.7 dB at the upper frequency of the operating band ($|\Gamma| = -10$ dB) and −21.6 dB at 2.45 GHz. For the elliptical radiator, the CPLH-P is −22.4 dB at 2.45 GHz and −20.7 dB at the upper frequency. On the other hand, for the triangular patch, the CPLH-P is −19.7 dB at 2.45 GHz and −18.0 dB at the lower frequency. The bandwidth of all new antennas remained close to 5.9%.

To conclude the analysis, normalized radiation patterns are shown in Figures 11 and 12. The copolarized patterns are equivalent to those presented in [40], except that the cross polarization (in the H-plane) is now minimized. Consequently, the antennas' directivity is similar, as illustrated in Table 2. The simulated results for the radiation efficiency, CPLH-P,

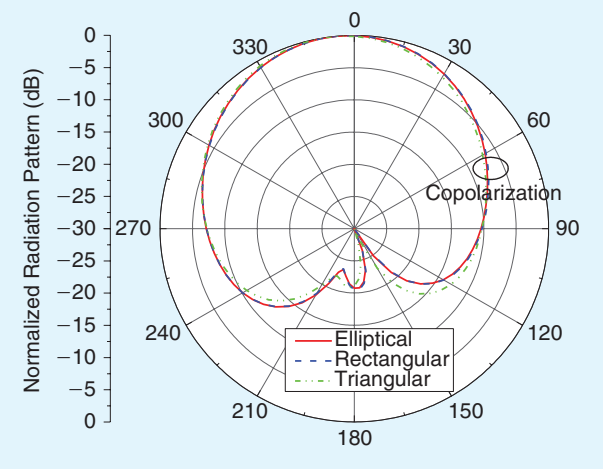

FIGURE 11. The E-plane normalized radiation pattern at 2.45 GHz.

bandwidth (BW), input impedance (Z_{in}), and ΔCP parameter are also shown in Table 2.

MUTUAL COUPLING ANALYSIS

With the electrically equivalent radiators designed per the criterion introduced in the "New Design Procedure" section, the analysis of mutual coupling can now be carried out in a more effective way. Arrays made out of two patches of equal geometries were simulated in HFSS for a fixed $\lambda_o/2$ displacement d between their geometric centers. Two arrangements were considered: the classical side-by-side configuration and the collinear one. Figures 13 and 14 illustrate these configurations in the case of rectangular patches—note that the geometric centers of the arrays coincide with the center of the rectangular grounded FR4 layer (160 mm × 100 mm). Simulations were performed in HFSS, at 2.45 GHz for six different arrays using the electrically equivalent microstrip antennas designed in the "New Design Procedure" section. The mutual coupling levels are shown in Table 3. The letters ***S*** and ***C*** indicate the array topology (side by side or collinear), and the index specifies the array elements: E for elliptical patch, R for rectangular, and T for triangular.

It is possible to establish a particular condition for low CPLH-P all over the antenna bandwidth.

As expected, the mutual coupling levels are equivalent since the radiators were designed to be electrically equivalent (according to the criterion proposed in this article). Note that the best value of mutual coupling was obtained for the $\boldsymbol{C}_E$ configuration, i.e., the collinear array of elliptical patches.

Broadside normalized radiation patterns in the H- and E-plane are shown in Figures 15 and 16 for the side-by-side and collinear configurations, respectively.

As the antennas are electrically equivalent, similar radiation patterns were obtained. However, back lobe for the side-by-side configuration is greater than that for the collinear one. This lobe occurs since the edge diffraction of the copolarized component is more intense in the side-by-side array. Moreover, this configuration is slightly more directive than the collinear one

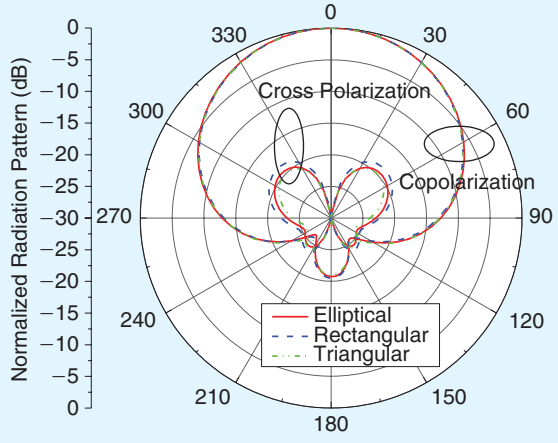

FIGURE 12. The H-plane normalized radiation pattern at 2.45 GHz.

TABLE 2. THE ELECTRICAL CHARACTERISTICS OF LP MICROSTRIP ANTENNAS.

	Rectangular	Elliptical	Triangular
Directivity (dB)	6.57	6.52	6.60
Radiation Efficiency (%)	77.3	76.4	76.7
CPLH-P (dB)	−21.6	−22.4	−19.7
Bandwidth at −10 dB (MHz)	143	135	146
Z_{in} (Ω)	130	130	50
ΔCP (dB)	−19.7–−21.6	−20.7–−22.4	−18.0–−19.7

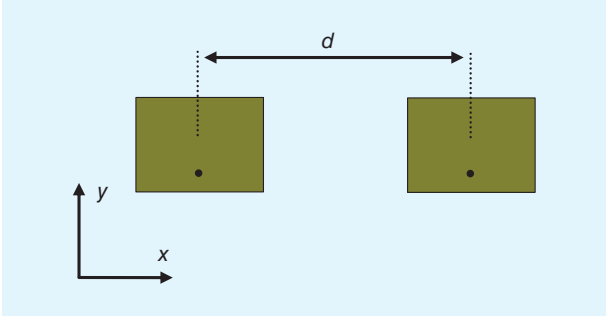

FIGURE 13. The side-by-side configuration.

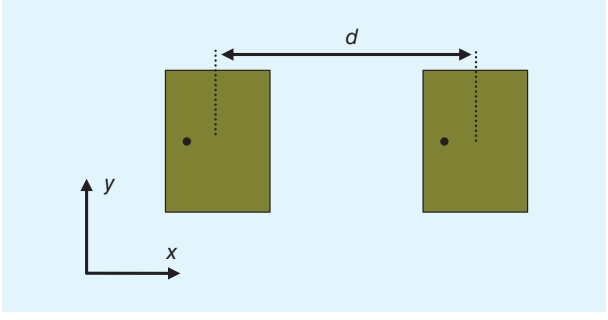

FIGURE 14. The collinear configuration.

TABLE 3. MUTUAL COUPLING BETWEEN ELECTRICALLY EQUIVALENT MICROSTRIP ANTENNAS.

Configuration	$\lvert S_{21}\rvert$ dB	Configuration	$\lvert S_{21}\rvert$ dB
$\boldsymbol{S}_E$	−20.5	$\boldsymbol{C}_E$	−21.0
$\boldsymbol{S}_R$	−20.4	$\boldsymbol{C}_R$	−20.8
$\boldsymbol{S}_T$	−19.9	$\boldsymbol{C}_T$	−20.0

(9.2 dB versus 8.9 dB). The arrays' cross polarization is better than −30 dB. Consequently, the collinear configuration was selected for implementation.

DESIGN OF A LOW-COST COLLINEAR ARRAY

As the antennas designed in the "New Design Procedure" section are electrically equivalent, any of the patches could be used in a low-cost collinear array. Therefore, rectangular patches were chosen because they are easy to simulate and build. As

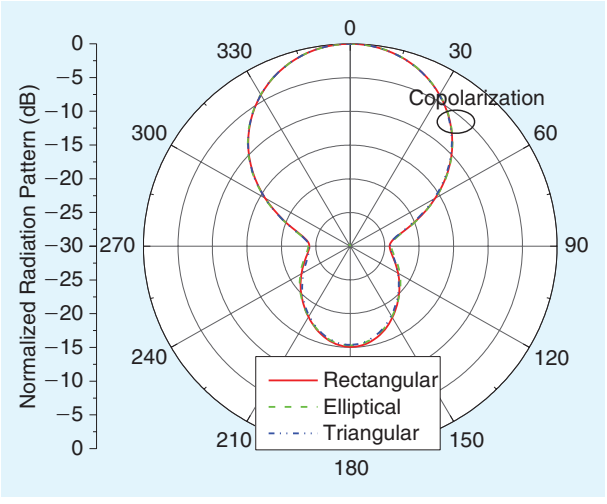

FIGURE 15. The H-plane normalized radiation pattern of the side-by-side array at 2.45 GHz.

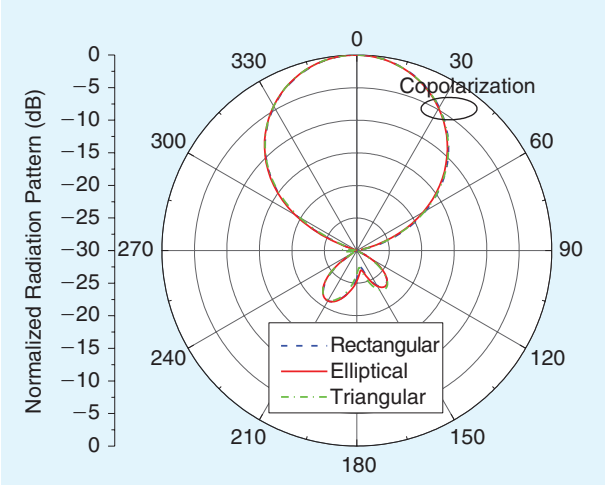

FIGURE 16. The E-plane normalized radiation pattern of the collinear array at 2.45 GHz.

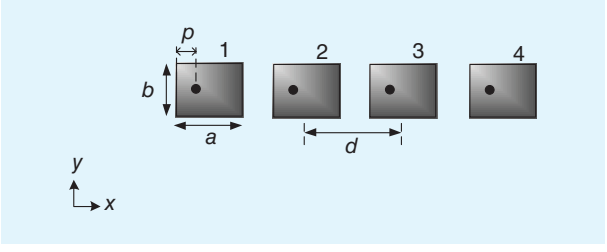

FIGURE 17. The collinear array of rectangular patches.

mentioned previously, the array has to comply with the following specifications: a 12-dB directivity in the broadside configuration, a −17-dB SLL, a −10-dB minimum reflection coefficient magnitude, and the CPLH-P as low as –20 dB, all over the ISM band (2.4–2.5 GHz). The specified directivity and SLL will determine the number of the array elements and the respective excitation coefficients. Since the solution is not unique, a homemade computer-aided design (CAD) based on the iterative solution of linearly constrained least square problems [43] was implemented. As usually assumed in preliminary design, mutual coupling effects were not considered, and the grounded dielectric layer under the patch was supposed to be infinite. This CAD produced the four-element array illustrated in Figure 17, with the following coefficients: $I_1 = 0.7\ A$, $I_2 = 1.0\ A$, $I_3 = 1.0\ A$, and $I_4 = 0.7\ A$. Simulations were thus carried out for rectangular patches with dimensions $a = 25.6$ mm, $b = 20.5$ mm, $p = 7.0$ mm, and $d = 60$ mm (close to $\lambda_0/2$ at 2.45 GHz), printed onto a 6.6-mm thick grounded FR4 substrate.

The CAD-simulated E-plane radiation pattern (Figure 18) shows that the SLL is −17 dB, as specified. In addition, the array directivity at 2.45 GHz is 12 dB. However, the HFSS simulation is required for the analysis of relevant effects, for which the homemade CAD does not account. The electrical parameters of a microstrip array, like its mutual coupling and radiation patterns, are dependent on the substrate thickness and electrical characteristics, dimensions of the grounded dielectric, and displacement and relative position of the patches. In the present case, the geometric center of the array is positioned to coincide with the center of the 150 mm × 330 mm rectangular grounded dielectric, as shown in Figure 19. Notice that, at this stage of the design, each array element is directly excited by a coaxial probe.

Simulated results for the radiation patterns in the E- and H-planes are presented in Figures 20 and 21. The array directivity is 12 dB, as specified, the radiation efficiency is 74%, the CPLH-P parameter is −22.9 dB, and the active input impedances are listed in Table 4. These impedances will guarantee

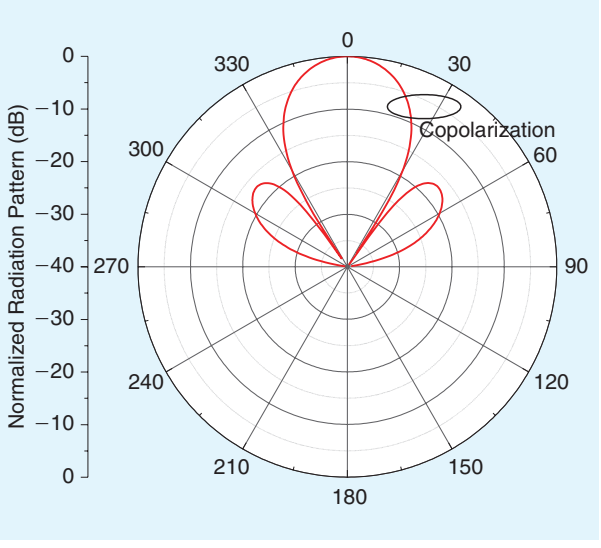

FIGURE 18. The E-plane normalized radiation pattern at 2.45 GHz.

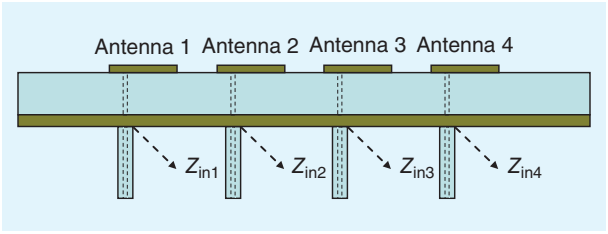

FIGURE 19. The geometry of the four-element array in HFSS.

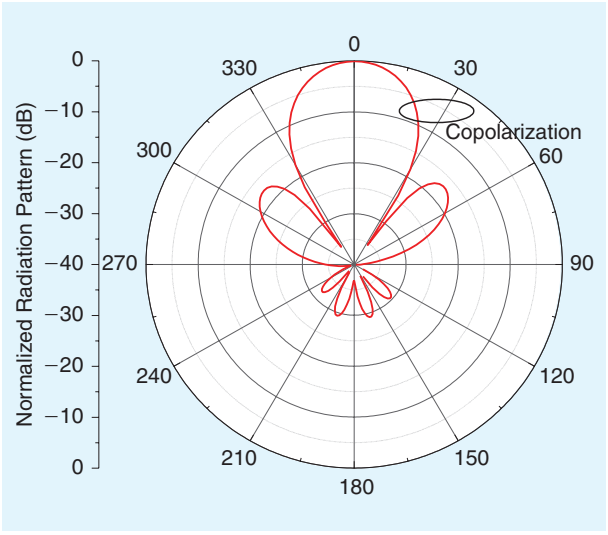

FIGURE 20. The E-plane normalized radiation pattern simulated in HFSS at 2.45 GHz.

low cross polarization in the H-plane radiation pattern, according to the design criterion presented in the "New Design Procedure" section. The cross-polarization behavior in frequency will be treated next, since the beamforming circuit can have a significant effect on it.

Given the active input impedance of the array elements, the next step is the beamforming design, taking into account two important aspects: dielectric losses and array bandwidth. Plain FR4 is not viable for beamforming circuits in microwaves due to its high losses [27], [44]. To overcome this undesired characteristic [45], suspended substrates (like that illustrated in Figure 22) have been utilized. This particular structure permits the design of suitable low-loss microstrip components in terms of width and junction topologies.

Having chosen the beamforming structure, the next step was the design of the transition between the printed antenna and the beamforming circuit. It is composed of a coaxial probe (radius = 0.65 mm; length = layer 1 + layer 2 thickness) and a microstrip line, as illustrated in Figure 23. It was designed for a 50-Ω input impedance at the end of the microstrip line. Figure 24 shows a schematic representation of the beamforming structure. Layer 1 is 6.6-mm thick, whereas layers 2 and 3 are each 1.6-mm thick.

Designing the beamforming circuit in HFSS to take into account the near-field effect led to the following dimensions for the rectangular patches: $a = 25.85$ mm, $b = 20.8$ mm,

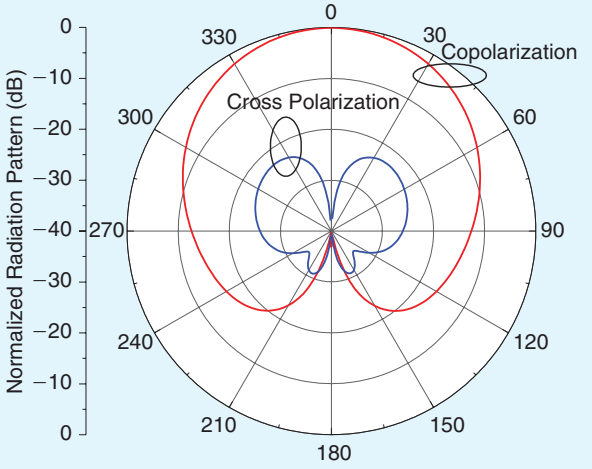

FIGURE 21. The H-plane normalized radiation pattern simulated in HFSS at 2.45 GHz.

TABLE 4. THE ACTIVE INPUT IMPEDANCES OF THE ARRAY ELEMENTS SIMULATED IN HFSS.

Z_{in1} (Ω)	Z_{in2} (Ω)	Z_{in3} (Ω)	Z_{in4} (Ω)
158 + *i* 44	152 + *i* 47	152 + *i* 47	161 + *i* 37

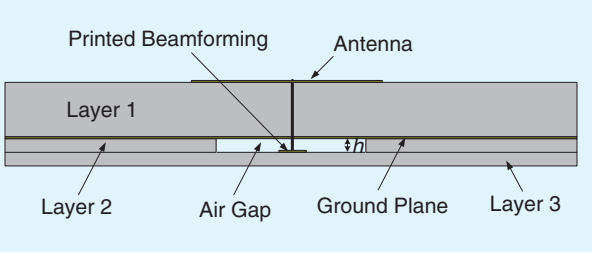

FIGURE 22. The cross section of the beamforming topology.

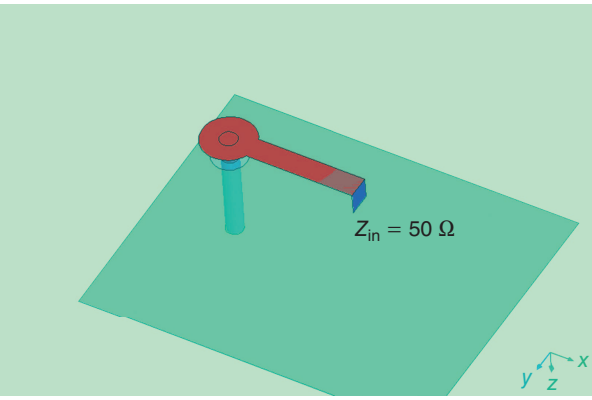

FIGURE 23. The transition between the antenna and the beamforming circuit.

and $p = 6.0$ mm. The radiation efficiency of the array fed by the beamforming circuit is 66%. Dimensions and characteristic impedances of the microstrip lines are available in [46],

TABLE 5. THE *S*-PARAMETERS OF THE BEAMFORMING CIRCUIT AT THE OPERATING CENTER FREQUENCY.

S_{11}	S_{21}	S_{31}	S_{41}	S_{51}
0, 13 ∠49°	0, 36 ∠−127°	0, 51 ∠−126°	0, 52 ∠−128°	0, 36 ∠−131°

whereas the beamforming *S*-parameters, simulated at the operating center frequency, are listed in Table 5.

As mutual coupling is now very low, the normalized *S*-parameters are close to the homemade CAD coefficients.

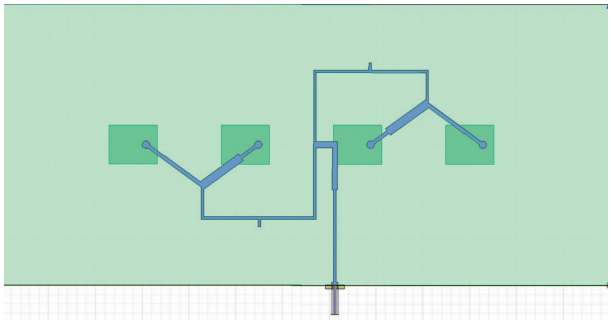

FIGURE 24. The schematic representation of the beamforming circuit.

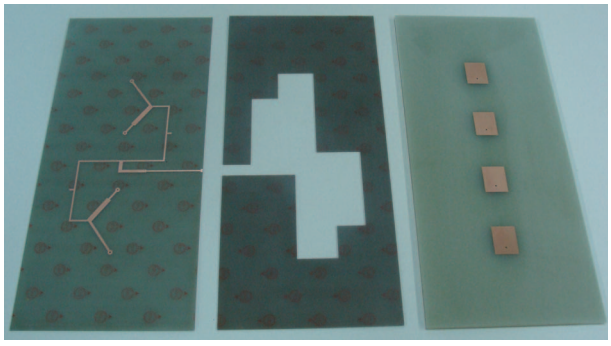

FIGURE 25. The pictures of the three layers that make up the collinear array.

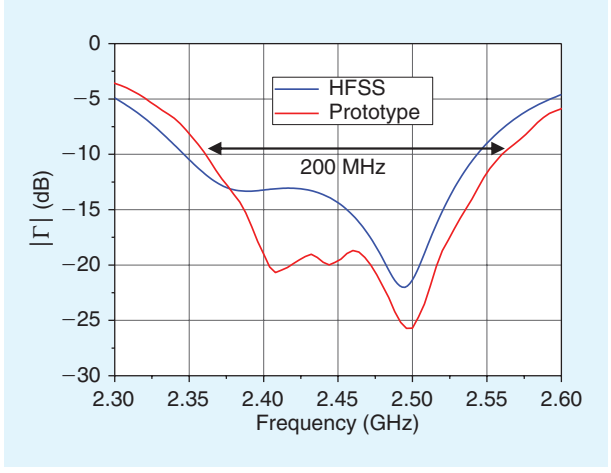

FIGURE 26. The reflection coefficient magnitude.

Note antennas 1, 2, 3, and 4 are positioned at ports 2, 3, 4, and 5, respectively.

The array prototype was manufactured with three FR4 layers, as illustrated in Figure 25. The beamforming circuit is shown on the left, printed onto a 1.6-mm thick layer. In the center is the spacer layer, also 1.6-mm thick. Note the cuts made for an air dielectric between the beamforming circuit and ground. Finally, the array printed onto a 6.6-mm thick layer is shown on the right.

The experimental and simulated results for the reflection coefficient magnitude are shown in Figure 26. As seen, the prototype bandwidth is 8.2% (200 MHz for a 10-dB return loss criterion), which properly covers the ISM band. Inaccuracy in relative permittivity, loss tangent, and thickness of the FR4 material [27] certainly causes the discrepancy observed in Figure 26. In the worst case, the simulated value is −13 dB, whereas the experimental value is −20 dB, i.e., the simulation indicates that 95% of the incident power is transmitted to the array, whereas the experimental result shows that 99% is transferred to the prototype. However, in the practical point of view, these values are similar.

To conclude the analysis, the experimental and simulated radiation patterns were compared. The results for the E-plane patterns are presented in Figure 27 and show excellent agreement. In addition, SLL is properly controlled under −17 dB, as specified.

Figure 28 shows the results for the H-plane. As expected, it is similar to the pattern for a single element. The cross-polarization pattern is no longer symmetrical due to the effects of the beamforming circuit. A very good agreement is observed between the simulated and the experimental patterns.

Measurements at other frequencies of the ISM band showed that the shape of the radiation patterns remained stable, but not the array's CPLH-P, as shown in Figure 29. However, the CPLH-P measurement is better than −21 dB,

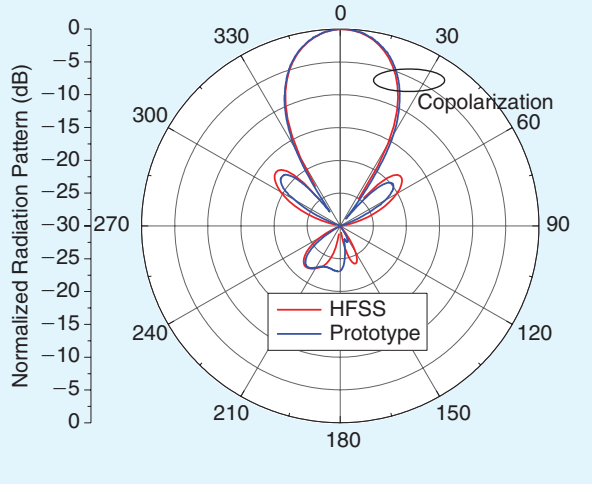

FIGURE 27. The E-plane normalized radiation pattern at 2.45 GHz.

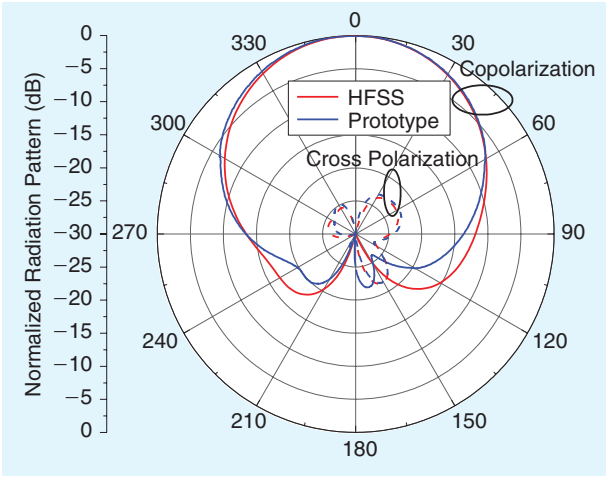

FIGURE 28. The H-plane normalized radiation pattern at 2.45 GHz.

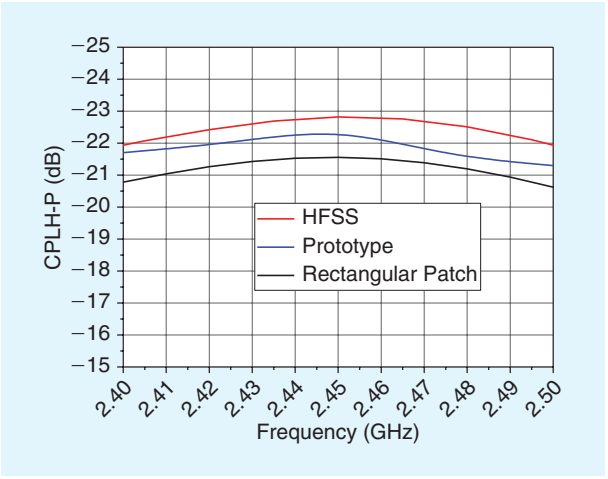

FIGURE 29. The H-plane cross-polarization level.

over the operating band, and the simulated and experimental curves are in good agreement.

CONCLUSION

A simple and efficient strategy for designing probe-fed electrically equivalent microstrip radiators on FR4 substrates was presented. This strategy was used for designing linearly-polarized rectangular, elliptical, and triangular patches, over the ISM band (2.4–2.5 GHz), with equivalent performance in terms of bandwidth, H-plane cross-polarization level, and resistive input impedance at the operating frequency. Consequently, their radiation patterns, directivity, and radiation efficiency were also shown to be substantially equivalent. Based on this strategy, mutual coupling between patches of equal geometry was analyzed, showing that electrically equivalent antennas are similar, despite the patch geometry. Similar results were obtained for the radiation patterns of broadside arrays of both side-by-side and collinear configurations.

To illustrate the proposed technique, a collinear array of rectangular patches was designed on an FR4 substrate: moderately thick for the patches, suspended from the beamforming circuit. Three steps were required. First, to comply with the specified directivity and SLL, the number of elements and their excitation coefficients were determined using a homemade CAD. Then, the array was simulated in HFSS to incorporate relevant effects that the homemade CAD does not. Finally, the beamforming was synthesized considering two important aspects: dielectric losses and array bandwidth. Per design requirements, the simulated radiation efficiency of the low-cost array was close to 70%. The experimental results for radiation patterns, CPLH-P, and reflection coefficient magnitude validate the proposed approach. In particular, the measured CPLH-P of the array was kept below −21 dB, which is over the operating band.

ACKNOWLEDGMENTS

We would like to thank Conselho Nacional de Desenvolvimento Científico e Tecnológico for sponsoring Project 402017/2013-7, Instituto de Fomento e Coordenação Industrial–Departamento de Ciência e Tecnologia Aeroespacial for the anechoic chamber, and Nilson Rabelo for the assistance in preparing this article. We would also like to thank the reviewers for their constructive comments and suggestions.

AUTHOR INFORMATION

D.C. Nascimento received his B.S. degree in telecommunications engineering from the Universidade de Taubaté, Brazil, in 2004, and his M.S. and Ph.D. degrees in electronics engineering from the Instituto Tecnológico de Aeronáutica (ITA), S.J. dos Campos, Brazil, in 2007 and 2013, respectively. His research interests include the area of electromagnetic theory and antennas, with an emphasis on microstrip antennas and arrays. He is currently an adjunct professor in the Department of Electronics Engineering, ITA.

J.C. da S. Lacava received his B.S. degree in electrical engineering from Faculdade de Engenharia de São José dos Campos, Brazil, in 1974, and his M.Sc. and Ph.D. degrees in electronics engineering from Instituto Tecnológico de Aeronáutica, S.J. dos Campos, Brazil, in 1979 and 1985, respectively. He was an adjunct researcher at the Instituto de Aeronáutica e Espaço, Brazil, from 1986 to 1987, an associate professor at Universidade da Beira Interior, Covilhã, Portugal, from 1992 to 1993, and a professor assistente doutor at the Universidade Estadual Paulista Júlio de Mesquita Filho, Faculdade de Engenharia de Guaratinguetá, Brazil, from 1993 to 1994. He is currently an associate professor and the head of the Laboratório de Antenas e Propagação of the Divisão de Engenharia Eletrônica, ITA, after serving as the head of the Departamento de Circuitos e Micro-ondas and the vice chair of the Divisão de Engenharia Eletrônica, ITA. His research interests include electromagnetic theory and antennas, with an emphasis on microstrip antennas and arrays.

REFERENCES

[1] R. Garg, P. Bhartia, I. Bahl, and A. Ittipiboon, *Microstrip Antenna Design Handbook*. Norwood, MA: Artech House, 2001.

[2] J. L. Volakis, Ed., *Antenna Engineering Handbook*, 4th ed. New York: McGraw-Hill, 2007.

[3] O. M. P. Filho, T. Ventura, C. Rego, A. S. Tinoco-S, and J. C. S. Lacava, "Cavity-backed cylindrical wraparound antennas," in *Microstrip Antennas*, Nasimuddin, Ed. Rijeka, Croatia: InTech, 2011, pp. 131–154.
[4] E. Chang, S. A. Long, and F. R. William, "An experimental investigation of electrically thick rectangular microstrip antennas," *IEEE Trans. Antennas Propag.*, vol. AP-34, no. 6, pp. 767–772, June 1993.
[5] P. S. Hall, "Probe compensation in thick microstrip patches," *Electron. Lett.*, vol. 23, no. 11, pp. 606–607, May 1987.
[6] M. J. Alexander, "Capacitive matching of microstrip antennas," *IEE Proc.*, vol. 137, pp. 172–174, Apr. 1989.
[7] P. S. Hall, J. S. Dahele, and P. M. Haskins, "Microstrip patch antennas on thick substrates," in *Proc. IEEE Int. Symp. Antennas Propagation*, San Jose, CA, June 1989, pp. 458–462.
[8] G. A. E. Vandenbosch and A. R. van de Capelle, "Study of the capacitively fed microstrip antenna element," *IEEE Trans. Antennas Propag.*, vol. AP-42, no. 12, pp. 1648–1652, Dec. 1994.
[9] P. M. Haskins and J. S. Dahele, "Capacitive coupling to patch antenna by means of modified coaxial connectors," *Electron. Lett.*, vol. 34, no. 23, pp. 2187–2188, Nov. 1998.
[10] P. L. Teng, C. L. Tang, and K. L. Wong, "A broadband planar patch antenna fed by a short probe feed," in *Proc. Asia-Pacific Microwave Conf.*, Dec. 2001, pp. 1243–1246.
[11] F. A. Chan and K. L. Wong, "A broadband probe-fed patch antenna with a thickened probe pin," in *Proc. Asia-Pacific Microwave Conf.*, Dec. 2001, pp. 1247–1250.
[12] Y. B. Tzeng, C. W. Su, and C. H. Lee, "Study of broadband CP patch antenna with its ground plane having an elevated portion," in *Proc. Asia-Pacific Microwave Conf.*, Dec. 2005.
[13] D. C. Nascimento, J. A. Mores Jr., R. Schildberg, and J. C. S. Lacava, "Low-cost truncated corner microstrip antenna for GPS application," in *Proc. IEEE Int. Symp. Antennas Propagation*, Albuquerque, NM, July 2006, pp. 1557–1560.
[14] D. C. Nascimento, I. Bianchi, R. Schildberg, and J. C. S. Lacava, "Design of probe-fed truncated corner microstrip antennas for globalstar system," in *Proc. IEEE Int. Symp. Antennas Propagation*, Honolulu, HI, June 2007, pp. 3041–3044.
[15] L. F. Marzall, D. C. Nascimento, R. Schildberg, and J. C. S. Lacava, "An effective strategy for designing probe-fed linearly-polarized thick microstrip arrays with symmetrical return loss bandwidth," *PIERS Online*, vol. 6, no. 8, pp. 700–704, 2010.
[16] A. S. Tinoco-S, D. C. Nascimento, R. Schildberg, and J. C. S. Lacava, "Analysis and design of rectangular microstrip antennas for educational purposes," *IEEE Antennas Propagat. Mag.*, vol. 53, no. 1, pp. 151–155, Feb. 2011.
[17] A. S. Tinoco-S, D. C. Nascimento, J. C. S. Lacava, and O. M. P. Filho, "Design of cavity-backed circularly-polarized cylindrical microstrip antennas," in *Proc. IEEE Int. Symp. Antennas Propagation*, Chicago, IL, July 2012, pp. 1–2.
[18] R. Gardelli, G. L. Cono, and M. Albani, "A low-cost suspended patch antenna for WLAN access points and point-to-point links," *IEEE Antennas Wireless Propagat. Lett.*, vol. 3, no. 1, pp. 90–93, 2004.
[19] R. Lelaratne and R. J. Langley, "Dual-band patch antenna for mobile satellite systems," *IEE Proc.—Microwave Antennas Propagat.*, vol. 147, no. 6, pp. 427–430, Dec. 2000.
[20] M. Niroojazi and M. N. Azarmanesh, "Practical design of single feed truncated corner microstrip antenna," in *Proc. 2nd Annu. Conf. Communication Networks Services Research*, Canada, May 2004, pp. 25–29.
[21] S.-Y. Ke, "Efficiency improvement of a circularly polarized microstrip antenna using a two-layer substrate," *WHAMPOA—An Interdisciplinary J.*, vol. 53, pp. 19–24, 2007.
[22] Y.-F. Lin, H.-M. Chen, and S.-C. Lin, "A new coupling mechanism for circularly polarized annular-ring patch antenna," *IEEE Trans. Antennas Propag.*, vol. AP-56, no. 1, pp. 11–16, Jan. 2008.
[23] D. Bhardwa and D. Bhatnagar, "Radiation from double notched square patch antenna on FR4 substrate," *J. Microwaves, Optoelectron. Electromagn. Applicat.*, vol. 7, no. 2, pp. 54–64, Dec. 2008.
[24] G. Immadi, M. S. R. S. Tejaswi, M. V. Narayana, N. A. Babu, G. Anupama, and K. V. Raviteja, "Design of coaxial fed microstrip patch antenna for 2.4 GHz bluetooth applications," *J. Emerging Trends Comput. Inform. Sci.*, vol. 2, no. 12, pp, 686–690, Dec. 2011.
[25] A. A. Qureshi, M. U. Afzal, T. Taqueer, and M. A. Tarar, "Performance analysis of FR-4 substrate for high frequency microstrip antennas," in *Proc. China-Japan Joint Microwave Conf.*, Hangzhou, China, Apr. 2011, pp. 1–4.
[26] D. C. Nascimento, R. Schildberg, and J. C. S. Lacava, "New considerations in the design of low-cost probe-fed truncated corner microstrip antennas for GPS applications," in *Proc. IEEE Int. Symp. Antennas Propagation*, Honolulu, HI, June 2007, pp. 749–752.
[27] M. J. Ammann, "A Comparison of some low cost laminates for antennas operating in the 2.45 GHz ISM band," in *Proc. IEE Colloq. Low Cost Antenna Technology.*, London, Feb. 1998, pp. 1–5.
[28] D. C. Nascimento, R. Schildberg, and J. C. S. Lacava, "Design of low-cost microstrip antennas for glonass applications," *PIERS Online*, vol. 4, no. 7, pp. 767–770, 2008.
[29] D. C. Nascimento, R. Schildberg, and J. C. S. Lacava, "Design of probe-fed circularly-polarized rectangular-patch thick microstrip antenna revisited," in *Proc. IEEE Int. Symp. Antennas Propagation*, Toronto, ON, Canada, July 2010, pp. 1–4.
[30] D. C. Nascimento and J. C. S. Lacava, "Design of low-cost probe-fed microstrip antennas," in *Microstrip Antennas*, Nasimuddin, Ed. Rijeka, Croatia: InTech, 2011, pp. 1–26.
[31] K. Ozenc, M. E. Aydemir, and A. Oncu, "Design of a 1.26 GHz high gain microstrip patch antenna using double layer with Airgap for satellite reconnaissance," in *Proc. 6th Int. Conf. Recent Advances Space Technologies*, Istanbul, Turkey, June 2013, pp. 499–504.
[32] W. Hong, K. H. Baek, and A. Goudelev, "Multilayer antenna package for IEEE 802.11ad employing ultralow-cost FR4," *IEEE Trans. Antennas Propag.*, vol. AP-60, no. 12, pp. 5932–5938, Dec. 2012.
[33] Z. N. Chen and M. Y. W. Chia, "Broad-band suspended probe-fed plate antenna with low cross-polarization levels," *IEEE Trans. Antennas Propag.*, vol. AP-51, no. 2, pp. 345–346, Feb. 2003.
[34] A. Petosa, A. Ittipibon, and N. Gagnon, "Suppression of unwanted probe radiation in wideband probe-fed microstrip patches," *Electron. Lett.*, vol. 35, no. 5, pp. 355–357, Mar. 1999.
[35] C. Kumar and D. Guha, "Nature of cross-polarized radiations from probe-fed circular microstrip antennas and their suppression using different geometries of defected ground structure (DGS)," *IEEE Trans. Antennas Propag.*, vol. AP-60, no. 1, pp. 92–101, Jan. 2012.
[36] C. A. Balanis, *Antenna Theory: Analysis and Design*, 3rd ed. New York: Wiley, 2005.
[37] D. F. Kelly and W. L. Stutzman, "Array antenna pattern modeling methods that include mutual coupling effects," *IEEE Trans. Antennas Propag.*, vol. AP-41, no. 12, pp. 1625–1632, Dec. 1993.
[38] D. Pozar and D. H. Schaubert, *Microstrip Antennas: The Analysis and Design of Microstrip Antennas and Arrays*. Piscataway, NJ: IEEE Press, 1995.
[39] R. C. Hansen, *Phased Array Antennas*. New York: Wiley, 1998.
[40] D. C. Nascimento and J. C. S. Lacava, "Probe-fed linearly-polarized electrically-equivalent microstrip antennas on FR4 substrates," *J. Microwaves, Optoelectron. Electromagn. Applicat.*, vol. 13, no. 1, pp. 55–66, 2014.
[41] HFSS. (2014, Feb. 27). [Online]. Available: http://www.ansys.com/Products/Simulation +Technology/Electromagnetics/High-Performance+Electronic+Design/ANSYS+HFSS
[42] Y. Hu, D. R. Jackson, J. T. Williams, S. A. Long, and V. R. Komanduri, "Characterization of the input impedance of the inset-fed rectangular microstrip antenna," *IEEE Trans. Antennas Propag.*, vol. AP-56, no. 10, pp. 3314–3318, Oct. 2008.
[43] C. Y. Tseng and L. J. Griffiths, "A simple algorithm to achieve desired patterns for arbitrary arrays," *IEEE Trans. Signal Process.*, vol. 40, no. 11, pp. 2737–2746, Nov. 1992.
[44] J. R. Aguilar, M. Beadle, P. T. Thompson, and M. W. Shelley, "The microwave and RF characteristics of FR4 substrates," in *Proc. IEE Colloq. Low Cost Antenna Technology*, London, Feb. 1998.
[45] J. Coonrod. (2012, Feb.). Circuit materials and high-frequency losses of PCBs. The PCB Magazine. Rogers Corporation. [Online]. Available: https://www.rogerscorp.com/documents/2244/acm/articles/Circuit-Materials-an-High-Frequency-Losses-of-PCBs.pdf
[46] D. C. Nascimento, "Microstrip antennas and arrays on thick substrates with control of main beam direction, side lobe level, and directivity," Ph.D. Dissertation, Technol. Inst. Aeronautics, Brazil, 2013.